ChemComm

COMMUNICATION

View Article Online
View Journal | View Issue

Cite this: *Chem. Commun.*, 2025, **61**, 11247

Received 27th January 2025,
Accepted 6th June 2025

DOI: 10.1039/d5cc00512d

rsc.li/chemcomm

DBU as base and ligand in phosphine-free ruthenium complexes for hydrogenation of CO_2†

Andrew Z. Preston, [a] Alexander S. Phearman, [a] Manuel Quiroz, [a] Sarah E. Flowers, [a] Nilakshi Devi, [b] Christopher M. Zall, [b] Eric S. Wiedner, *[a] Aaron M. Appel [a] and John C. Linehan *[a]

In the presence of DBU base, ruthenium piano stool complexes catalyze the hydrogenation of CO_2 to formate at room temperature without phosphine ligands. Thermodynamic and kinetic studies reveal the active catalyst is formed by binding DBU as a ligand.

The catalytic hydrogenation of carbon dioxide is of interest for production of organic hydrogen carriers using an abundant and renewable carbon feedstock. Compared to molecular hydrogen, products such as formic acid, formate salts, and methanol formed from the hydrogenation of CO_2 are safer and easier to transport,[1–5] making them more suitable for temporary storage of hydrogen generated from intermittent energy sources.

Transition-metal complexes are effective catalysts for hydrogenation of CO_2 to formate/formic acid,[6–9] though many contain phosphine ligands that are prone to oxidation and are often challenging to synthesize. Some of the most active catalysts for hydrogenation of CO_2 to formate are the phosphine-free $[Cp^*Ir(L)(H_2O)]^+$ (L = *N*,*N*-bidentate ligand) family of complexes.[10–12] Other phosphine-free catalysts include complexes of Ru,[13–16] Co,[17,18] Fe,[19] and Mn,[20] typically possessing either pyridyl or N-heterocyclic carbene ligands.

Watari and Ikariya demonstrated that simple copper salts of the amidine base DBU (1,8-diazabicyclo[5.4.0]undec-7-ene) are catalysts for hydrogenation of CO_2 to formate (Fig. 1a).[21,22] In this example, DBU serves as both the ligand as well as the more typical role of exogenous base.[23–25] Subsequent reports showed that DBU binding to copper phosphine complexes, $Cu(PCP)(DBU)^+$ and $Cu(triphos)(DBU)^+$, also afforded catalysts for CO_2 hydrogenation.[26–29] Examples of DBU binding during catalytic reactions are sparse and typically lead to inhibition or decomposition of the catalyst, such as in C–N[30–32] and C–C[33,34] cross-coupling reactions. Therefore, these copper catalysts are notable for their ability to operate in the presence of DBU binding. However, relative to typical phosphine-based catalysts, the phosphine-free catalyst, $Cu(DBU)_2X$, exhibits a very low activity (TOF ~ 1 h^{-1} at 80 °C).[22] As a result, it remains unclear whether DBU is an effective supporting ligand for catalysis.

We report the hydrogenation of CO_2 to formate by $[CpRu(MeCN)_3]^+$ (**1**) and $[Cp^*Ru(MeCN)_3]^+$ (**2**), and demonstrate the essential role of DBU binding in this process. Both **1** and **2** are commercially available and forego phosphine ligands common for ruthenium-based CO_2 hydrogenation catalysts. Kinetic, thermodynamic, and spectroscopic experiments suggest that the precatalysts are activated by the reversible binding of up to two DBU ligands (Fig. 1b), resulting in highly active phosphine-free catalysts under mild conditions.

Complexes **1** and **2** were screened for activity in the catalytic hydrogenation of CO_2 with DBU. Addition of DBU (0.6 M) to a CD_3CN solution of **1** or **2** resulted in an immediate color change from bright yellow to red-orange. This solution was transferred

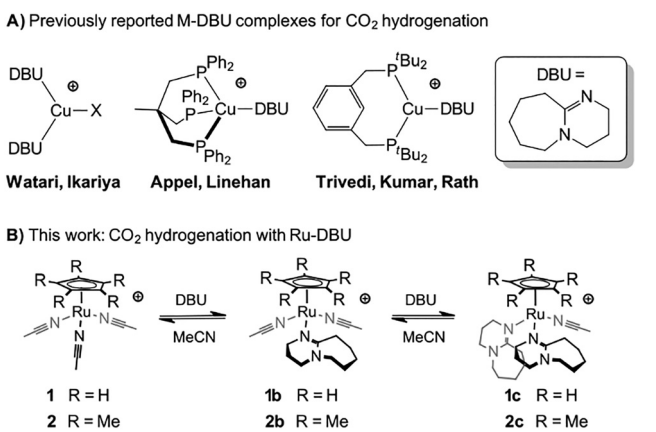

Fig. 1 (A) Examples of previously reported phosphine-free catalysts for CO_2 hydrogenation. (B) This work shows that Ru piano-stool complexes generate active CO_2 hydrogenation catalysts upon binding DBU as ligand.

[a] *Institute for Integrated Catalysis, Pacific Northwest National Laboratory, P.O. Box 999, Richland, Washington 99352, USA. E-mail: eric.wiedner@pnnl.gov, john.linehan@pnnl.gov*

[b] *Department of Chemistry, Sam Houston State University, Huntsville, Texas 77341, USA*

† Electronic supplementary information (ESI) available: Experimental data, kinetic data, spectral data, additional crystallographic data. CCDC 2329534. For ESI and crystallographic data in CIF or other electronic format see DOI: https://doi.org/10.1039/d5cc00512d

to a custom PEEK NMR tube,[35,36] pressurized with H_2/CO_2, and the reaction was monitored using high-pressure *operando* ^{1}H NMR spectroscopy. At 25 °C and 34 atm of 1 : 1 H_2/CO_2, both catalysts exhibited a steady rate of conversion to formate (Fig. 2a), with **1** exhibiting a higher rate (0.45 M h^{-1}) than **2** (0.1 M h^{-1}).

To determine the catalytic rate law for **2**, the initial turnover frequency (TOF) for catalysis was measured under varying conditions (Table S1, ESI†). Doubling [**2**] from 0.45 mM to 0.9 mM led to a 2× increase in the initial rate of formate production and no change in the TOF, consistent with a first-order dependence in the catalyst concentration. The dependence on base was determined using four different initial concentrations of DBU (0.3 M, 0.6 M, 0.9 M, 1.2 M) at 25 °C and 34 atm of 1 : 1 H_2/CO_2. A linear correlation was observed between the TOF and the initial DBU concentration (Fig. 2b), indicating a first-order dependence on DBU.

The reaction order in H_2 and CO_2 was tested by performing catalysis with **2** at varying pressures and ratios of the two gases with 0.6 M DBU at 25 °C.[37] The resulting TOF values showed saturation behavior in P_{H_2}, where the TOF is dependent on H_2 at low pressures and independent at higher pressures (Fig. 2c). No apparent dependence on P_{CO_2} was observed, with the 1 : 3 H_2/CO_2 gas mixture giving the second lowest TOF despite having the highest P_{CO_2} of 30 atm.

The possibility of DBU binding to Ru was first explored for **1** since the Cp ligand resonances are well-separated from those for DBU in the ^{1}H NMR spectrum. Upon mixing a sample of **1** and DBU (<50 mM) in CD_3CN, the formation of a second cyclopentadienyl species was observed by ^{1}H, $^{13}C\{^1H\}$, and gHMBC NMR spectroscopy (Fig. 3 and Fig. S13–S18, ESI†).

Additionally, new DBU resonances were observed downfield of the small resonances for free DBU, integrating to 1 DBU per new Cp-containing species by ^{1}H and quantitative $^{13}C\{^1H\}$ NMR spectroscopy. No NH resonance for $DBU(H)^+$ was observed. These spectra are consistent with 91% conversion to $[CpRu(DBU)(MeCN)_2]^+$ (**1b**) with 25 mM DBU.

Higher concentrations of DBU (100 or 313 mM) resulted in the disappearance of **1** and the appearance of $[CpRu(DBU)_2(MeCN)]^+$ (**1c**) (Fig. 3 and Fig. S19, ESI†). In ^{1}H NMR spectra at 25 °C, the Cp resonances for **1b** and **1c** were noticeably broadened as [DBU] increased, consistent with ligand exchange that is occurring on the NMR time scale. At lower temperatures of −35 °C to −10 °C, sharp well-defined peaks are observed for **1b** and **1c** (Fig. S42, ESI†). Quantitative $^{13}C\{^1H\}$ NMR spectroscopy with 1.3 M DBU at −35 °C confirmed the presence of two magnetically equivalent DBU ligands per Cp ring in **1c** (Fig. S20, ESI†). The exchange rate between **1b** and **1c** increases with the temperature and concentration of DBU, and the species coalesce into a single peak by 25 °C with 1.3 M DBU. An absolute rate of 29 s^{-1} at 25 °C was calculated for exchange between **1b** and **1c** using the peak shapes (Fig. S21–S30 and Table S2, ESI†). This rate of ligand exchange is very fast relative to the timescale of catalytic CO_2 hydrogenation (0.03–0.2 s^{-1} at 25 °C).

Similar to **1**, a solution of **2** (25 mM) and DBU (25 mM) gave rise to shifted Cp* and DBU resonances. 1-D and 2-D ^{1}H and ^{13}C NMR spectroscopy and quantitative $^{13}C\{^1H\}$ NMR spectroscopy experiments are consistent with 83% conversion to $[Cp^*Ru(DBU)(MeCN)_2]^+$ (**2b**) at 25 °C (Fig. S31 and S32, ESI†). With 100 mM DBU, 97% conversion to **2b** is observed by ^{1}H NMR spectroscopy. Higher [DBU] obscures the Cp* peak in the ^{1}H NMR spectrum, but $^{13}C\{^1H\}$ NMR spectra with higher [DBU] show full conversion of **2** to **2b** (Fig. S32–S36, ESI†). Compared to the CpRu speciation at the same [DBU], the Cp*Ru species requires higher [DBU] to fully form $[Cp^*Ru(DBU)(MeCN)_2]^+$. No formation of $[Cp^*Ru(DBU)_2(MeCN)]^+$ (**2c**) is

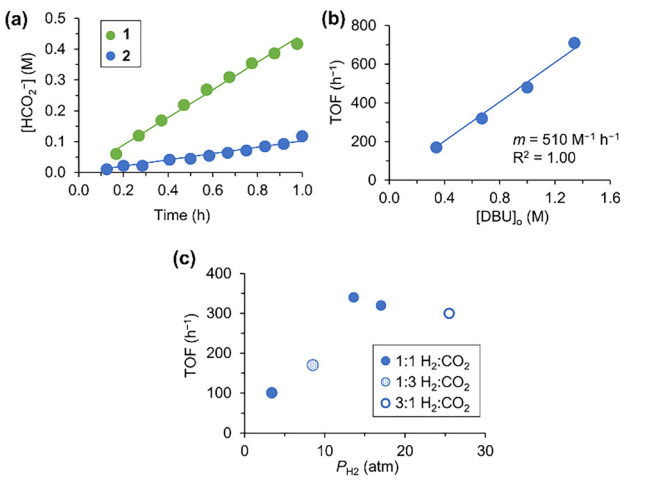

Fig. 2 (a) Conversion of CO_2 to formate by **1** and **2**. Conditions: 0.5 mM **1**/**2**, 600 mM DBU, 17 atm H_2/17 atm CO_2 at 25 °C in CD_3CN. (b) Plot of the DBU dependence on the TOF for **2** (17 atm H_2/17 atm CO_2, 25 °C). (c) Plot of the H_2 dependence on the TOF for **2** ($[DBU]_o$ = 0.61–0.67 M, 25 °C).

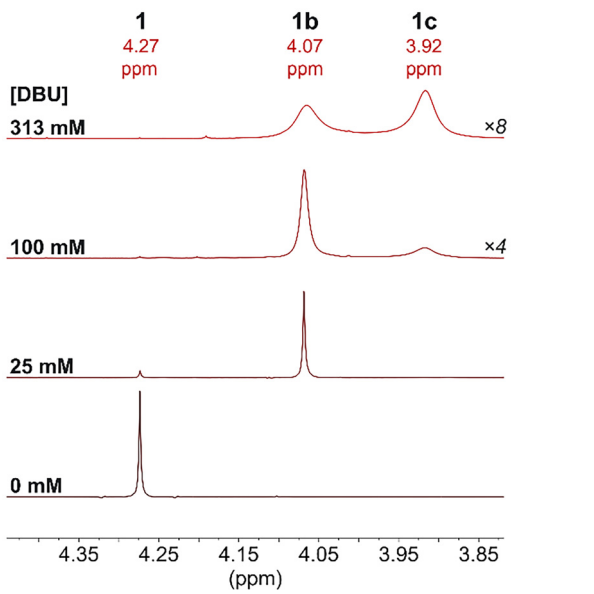

Fig. 3 ^{1}H NMR spectrum (500 MHz, CD_3CN, 25 °C) of the Cp resonance of **1** (25 mM) with varying [DBU]. Spectra with 100 and 313 mM DBU are magnified ×4 and ×8, respectively, due to significant broadening of the Cp signals.

observed until much higher DBU concentrations are used (Fig. S37 and S38, ESI†). Quantitative $^{13}C\{^1H\}$ NMR spectra of **2** in a mixture of 6.04 M DBU and 2.14 M CD_3CN at −35 °C, necessary to reduce broadening from ligand exchange, show 45% conversion to **2c**.

The identity of **2b** was further confirmed by X-ray diffraction studies. Single crystals of **2b** were grown by vapor diffusion of Et_2O into a DBU/MeCN solution of the Ru species (Fig. 4). This is the first reported structure of a Ru–DBU complex.[38]

Thermodynamic parameters for binding the DBU ligands were determined from Van't Hoff plots (Table S7, Fig. S40–S44, ESI†). The binding enthalpy of the first DBU (ΔH_1°) was found to be nearly identical for **1** (−6.9 kcal mol^{-1}) and **2** (−7.2 kcal mol^{-1}), while the entropy of binding (ΔS_1°) was lower for **2** (−4.6 cal mol^{-1} K^{-1}) than for **1** (0.2 cal mol^{-1} K^{-1}). As a result, K_1 at 25 °C is larger for **1** (1.2×10^5) than for **2** (1.8×10^4). These results indicate the first DBU binding is enthalpically driven with **2b** having a slight entropic penalty, potentially due to restricted motion of the DBU ligand caused by steric interactions with Cp*.

The equilibrium for binding the second DBU exhibited a more pronounced difference between **1b** and **2b**. The binding enthalpy for the second DBU (ΔH_2°) is exothermic for **1b** (−4.1 kcal mol^{-1}) but endothermic for **2b** (3.7 kcal mol^{-1}). In addition, the entropy of binding (ΔS_2°) changes from negative for **1b** (−5.5 cal mol^{-1} K^{-1}) to positive for **2b** (12 cal mol^{-1} K^{-1}). At 25 °C, K_2 is nearly two orders of magnitude larger for **1b** (66) than for **2b** (0.9). These large differences in ΔH_2° and ΔS_2° suggest that the CH_3CN ligand of **2c** may be much more labile than in **1c** (see ESI†); however, this could not be confirmed with the available data due to the low equilibrium population of **2c**.

The measured binding constants indicate **2** is a precatalyst that rapidly binds DBU to generate a mixture of **2b** (97%) and **2c** (3%) under catalytic conditions. The kinetic data is most consistent with **2b** being the active catalyst form according to the mechanism in Scheme 1. From the **2b** resting state, catalysis proceeds by pre-equilibrium binding of H_2 to give a dihydrogen complex, $[Cp^*Ru(H_2)(DBU)(CH_3CN)]^+$ (**2b-H2**). Rate-limiting deprotonation by exogenous DBU to form $Cp^*Ru(H)(DBU)(CH_3CN)$ (**2b-H**) and a protonated base then occurs. The cycle is completed by rapid hydride transfer from **2b-H** to CO_2 to yield **2b** and formate.

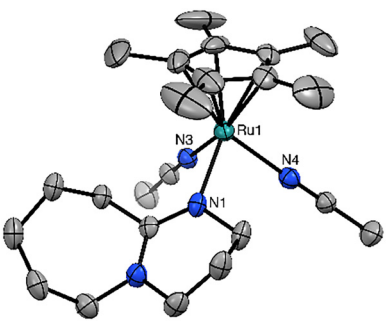

Fig. 4 Solid state structure of **2b** as determined by X-ray crystallography. Hydrogen atoms and the PF_6 anion are omitted for clarity. Thermal ellipsoids are shown at 50% probability.

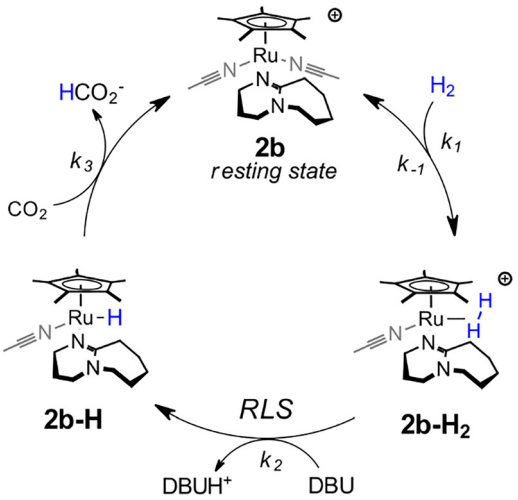

Scheme 1 Proposed catalytic cycle for hydrogenation of CO_2 to formate by **2**.

Catalysis could also occur through an alternative cycle involving two DBU ligands, but the first-order dependence on [DBU] indicates such a cycle is not kinetically competitive for **2**. This could be due to its unfavorable equilibrium for binding a second DBU ligand. Under catalytic conditions, **2c** constitutes only 3–7% of the total Ru species. It is noteworthy that **1** exhibits both a higher initial population of the bis-DBU adduct (70%) and a higher TOF, potentially consistent with a secondary catalytic cycle involving coordination of two DBU ligands.

Phosphine-free molecular catalysts for CO_2 hydrogenation are relatively uncommon and typically require high temperatures and pressures.[6,7] The most active phosphine-free catalysts, $[Cp^*Ir(L)(H_2O)]^+$ (L = *N*,*N*-bidentate ligand), display initial TOFs as high as 200 h^{-1} under ambient conditions (25 °C, 1 atm) in aqueous $NaHCO_3$ solution.[39] Catalyst **2** displays a comparable TOF of 100 h^{-1} under slightly more forcing conditions (25 °C, 6.8 atm) using DBU as the base in MeCN solution.

Higher TOFs are obtained for phosphine-based ruthenium catalysts at elevated temperatures and pressures. For example, a Ru(PNP) pincer complex exhibits a TOF of 36 000 h^{-1} (65 °C, 40 atm, 1.1 M DBU).[40] A more direct comparison with **2** can be made by extrapolating the temperature-dependent TOF of the Ru(PNP) catalyst to a value of 9400 h^{-1} at 25 °C with 40 atm of 3 : 1 H_2 : CO_2 (Fig. S45, ESI†).[41] Under similar conditions (1.3 M DBU, 34 atm 1 : 1 H_2 : CO_2), **2** affords a TOF of 710 h^{-1}. Normalizing for the difference in pressure suggests **2** is within an order of magnitude of the activity of Ru(PNP). This modest difference is quite remarkable since **2** does not rely on phosphine ligands, but rather uses the simple DBU base as a ligand.

In conclusion, we observed that the phosphine-free complexes $[CpRu(MeCN)_3]^+$ and $[Cp^*Ru(MeCN)_3]^+$ are active precatalysts for the hydrogenation of CO_2 to formate with DBU base. Mechanistic studies reveal the key role of coordination of DBU as an ancillary ligand in the active species. Detailed studies of the catalytic mechanism revealed the rate determining step is the heterolytic cleavage of a Ru–H_2 complex to form the subsequent hydride and a protonated base.

This work was supported by the U.S. Department of Energy, Office of Science, Office of Basic Energy Sciences, Chemical Sciences, Geosciences & Biosciences Division, Catalysis Science program, FWP 47319. Work by C. M. Z. and N. D. was supported by the U.S. Department of Energy, Office of Science, Office of Workforce Development for Teachers and Scientists (WDTS) under the Visiting Faculty Program (VFP), as well as by Sam Houston State University through the Faculty Research Grant.

Conflicts of interest

There are no conflicts to declare.

Data availability

The data supporting this article have been included as part of the ESI.† Crystallographic data for **2b** has been deposited at the CCDC under the number 2329534.†

Notes and references

1 A. Kumar, P. Daw and D. Milstein, *Chem. Rev.*, 2022, **122**, 385–441.
2 R. Sen, A. Goeppert and G. K. Surya Prakash, *Angew. Chem., Int. Ed.*, 2022, **61**, e202207278.
3 S. Chatterjee, I. Dutta, Y. Lum, Z. Lai and K.-W. Huang, *Energy Environ. Sci.*, 2021, **14**, 1194–1246.
4 K. Grubel, H. Jeong, C. W. Yoon and T. Autrey, *J. Energy Chem.*, 2020, **41**, 216–224.
5 S. Enthaler, J. von Langermann and T. Schmidt, *Energy Environ. Sci.*, 2010, **3**, 1207–1217.
6 W.-H. Wang, Y. Himeda, J. T. Muckerman, G. F. Manbeck and E. Fujita, *Chem. Rev.*, 2015, **115**, 12936–12973.
7 K. Sordakis, C. Tang, L. K. Vogt, H. Junge, P. J. Dyson, M. Beller and G. Laurenczy, *Chem. Rev.*, 2018, **118**, 372–433.
8 P. G. Jessop, T. Ikariya and R. Noyori, *Chem. Rev.*, 1995, **95**, 259–272.
9 W. Wang, S. Wang, X. Ma and J. Gong, *Chem. Soc. Rev.*, 2011, **40**, 3703–3727.
10 J. F. Hull, Y. Himeda, W. H. Wang, B. Hashiguchi, R. Periana, D. J. Szalda, J. T. Muckerman and E. Fujita, *Nat. Chem.*, 2012, **4**, 383–388.
11 R. Kanega, N. Onishi, D. J. Szalda, M. Z. Ertem, J. T. Muckerman, E. Fujita and Y. Himeda, *ACS Catal.*, 2017, **7**, 6426–6429.
12 A. Nijamudheen, R. Kanega, N. Onishi, Y. Himeda, E. Fujita and M. Z. Ertem, *ACS Catal.*, 2021, **11**, 5776–5788.
13 S. Ogo, R. Kabe, H. Hayashi, R. Harada and S. Fukuzumi, *Dalton Trans.*, 2006, 4657–4663.
14 H. Hayashi, S. Ogo and S. Fukuzumi, *Chem. Commun.*, 2004, 2714–2715.
15 A. Weilhard, S. P. Argent and V. Sans, *Nat. Commun.*, 2021, **12**, 231.
16 A. Weilhard, K. Salzmann, M. Navarro, J. Dupont, M. Albrecht and V. Sans, *J. Catal.*, 2020, **385**, 1–9.
17 Y. M. Badiei, W.-H. Wang, J. F. Hull, D. J. Szalda, J. T. Muckerman, Y. Himeda and E. Fujita, *Inorg. Chem.*, 2013, **52**, 12576–12586.
18 W. Yao, G. Olajide, C. M. Boudreaux, M. M. Wysocki, M. K. Ahmed, F. Qu, T. Szilvási and E. T. Papish, *Organometallics*, 2024, **43**, 1447–1458.
19 S. Coufourier, Q. Gaignard Gaillard, J.-F. Lohier, A. Poater, S. Gaillard and J.-L. Renaud, *ACS Catal.*, 2020, **10**, 2108–2116.
20 A. Dubey, L. Nencini, R. R. Fayzullin, C. Nervi and J. R. Khusnutdinova, *ACS Catal.*, 2017, **7**, 3864–3868.
21 R. Watari, S. Kuwata and Y. Kayaki, *Chem. Lett.*, 2020, **49**, 252–254.
22 R. Watari, Y. Kayaki, S. Hirano, N. Matsumoto and T. Ikariya, *Adv. Synth. Catal.*, 2015, **357**, 1369–1373.
23 S. Kostera, S. Weber, M. Peruzzini, L. F. Veiros, K. Kirchner and L. Gonsalvi, *Organometallics*, 2021, **40**, 1213–1220.
24 C. M. Hert, J. B. Curley, S. P. Kelley, N. Hazari and W. H. Bernskoetter, *Organometallics*, 2022, **41**, 3332–3340.
25 J. Hu, Q. J. Bruch and A. J. M. Miller, *J. Am. Chem. Soc.*, 2021, **143**, 945–954.
26 M. Trivedi, A. Kumar, A. Husain and N. P. Rath, *Inorg. Chem.*, 2021, **60**, 4385–4396.
27 R. R. Persaud, Z. Fang, C. M. Zall, A. M. Appel and D. A. Dixon, *J. Phys. Chem. A*, 2021, **125**, 6600–6610.
28 C. M. Zall, J. C. Linehan and A. M. Appel, *J. Am. Chem. Soc.*, 2016, **138**, 9968–9977.
29 C. M. Zall, J. C. Linehan and A. M. Appel, *ACS Catal.*, 2015, **5**, 5301–5305.
30 L. Fan and O. V. Ozerov, *Chem. Commun.*, 2005, 4450–4452.
31 N. Kumagai, S. Matsunaga and M. Shibasaki, *J. Am. Chem. Soc.*, 2004, **126**, 13632–13633.
32 N. Kumagai, S. Matsunaga and M. Shibasaki, *Tetrahedron*, 2007, **63**, 8598–8608.
33 R. Y. Liu, J. M. Dennis and S. L. Buchwald, *J. Am. Chem. Soc.*, 2020, **142**, 4500–4507.
34 J. M. Dennis, N. A. White, R. Y. Liu and S. L. Buchwald, *ACS Catal.*, 2019, **9**, 3822–3830.
35 C. R. Yonker and J. C. Linehan, *Prog. Nucl. Magn. Reson. Spectrosc.*, 2005, **47**, 95–109.
36 C. R. Yonker and J. C. Linehan, *J. Organomet. Chem.*, 2002, **650**, 249–257.
37 Z. K. Lopez-Castillo, S. N. V. K. Aki, M. A. Stadtherr and J. F. Brennecke, *Ind. Eng. Chem. Res.*, 2008, **47**, 570–576.
38 C. R. Groom, I. J. Bruno, M. P. Lightfoot and S. C. Ward, *Acta Crystallogr., Sect. B: Struct. Sci., Cryst. Eng. Mater.*, 2016, **72**, 171–179.
39 R. Kanega, M. Z. Ertem, N. Onishi, D. J. Szalda, E. Fujita and Y. Himeda, *Organometallics*, 2020, **39**, 1519–1531.
40 G. A. Filonenko, R. van Putten, E. N. Schulpen, E. J. M. Hensen and E. A. Pidko, *ChemCatChem*, 2014, **6**, 1526–1530.
41 G. A. Filonenko, E. J. M. Hensen and E. A. Pidko, *Catal. Sci. Technol.*, 2014, **4**, 3474–3485.

